Model predictive control of a continuous, nonlinear, two-phase reactor

N. Lawrence Ricker*

Department of Chemical Engineering, BF-10, University of Washington, Seattle, WA 98195, USA

Received 11 February 1993; revised 14 May 1993

The Tennessee Eastman challenge problem is simplified to a plant with eight states, four manipulated variables, and 10 outputs. Six regulation/optimization scenarios are proposed. The modified problem retains nonlinearities that cause difficulties in the original, e.g. certain gains can change sign. Steady-state relative-gain analysis suggests variable pairings for multi-loop feedback control that turn out to be inappropriate. A more robust, near-optimal multi-loop design is proposed and tested in simulations. Two model predictive control (MPC) designs are also tested. The first is based on a linear time-invariant (LTI) model of all the plant interactions. Gain variations make it impossible to achieve acceptable performance. The second uses a LTI model in which 10 of the 16 transfer functions are zero, i.e. it includes only the most important plant responses. The resulting MPC performance is comparable or better than the multi-loop design. Alternative MPC strategies are also discussed.

Keywords: predictive control; nonlinear reactor; decentralized control

In response to repeated requests from the process control research community, challenge problems have been published recently by four different industrial research groups. These differ markedly. For example, the problem proposed by Shell[1] is a set of transfer functions representing a crude fractionator, and model uncertainty is specified as bounded gain variations. The statement of the problem leads naturally to a solution via model predictive control (MPC) and related techniques, although other methods have been proposed and appear to be competitive[2]. The problem proposed by Chylla and Haase[3] is a single-input, single-output (SISO), nonlinear, semi-batch reactor. An MPC solution has been provided by Gattu and Zafiriou[4], who repeatedly linearized the governing equations during a batch run to update the linear model used in MPC. A similar strategy was used earlier by Garcia to control an industrial polymerization process[5].

The other two problems are multi-input, multi-output (MIMO), continuous processes, represented by mechanistic dynamic models. The Amoco problem involves control of a fluidized catalytic cracker (FCC) and regenerator[6]. Model equations are published, and a simulation is available for testing alternative control strategies. A response to this specific problem has yet to be published, but researchers have proposed strategies for similar FCC processes (e.g. Reference 7).

*E-mail: RICKER@CHEME.WASHINGTON.EDU)

The Tennessee Eastman (TE) problem requires coordination of three unit operations: an exothermic, two-phase reactor, a flash separator and a reboiled stripper[8]. There are 41 measured output variables (with added measurement noise) and 12 manipulated variables. Although FORTRAN code representing the process is available from the authors, they have chosen not to publish the model equations. Instead, they provide a flowsheet, a steady-state material balance, and a qualitative description of the key process characteristics. Part of the challenge is to decipher what is going on from the limited information provided. I was intrigued by this, as well as the plant-wide flavour of the problem. It seemed to represent an interesting case study for MPC.

It turned out to be more interesting than expected. Conventional multiloop approaches worked reasonably well, but a centralized MPC design was difficult to stabilize. Certain disturbances and setpoint changes caused severe degradation of control quality, e.g. violation of specified shutdown limits on pressure and liquid level in the reactor. The problem was so complex, however, that the reasons for the observed behaviour were obscure.

This was the motivation for the present work, which considers a simplified version of the TE problem. The first section of the paper describes the simplified process and a model that contains eight state variables, four manipulated variables and 10 measured outputs. Next,

0959–1524/93/020109–15

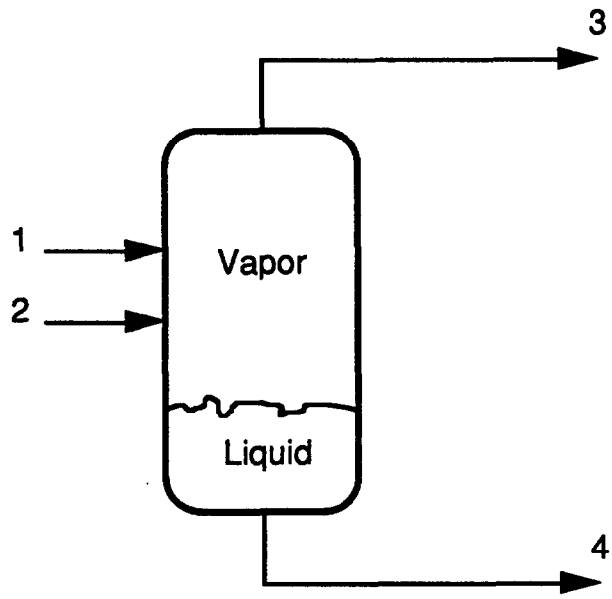

Figure 1 Process schematic

six operating scenarios are proposed and control strategies developed. These include conventional multiloop PID, and several MPC variants. A centralized, 'plant-wide' application of MPC leads to the same robustness problems observed in the original TE case study. Here, however, it is easier to isolate the cause. Several solutions are proposed and their relative merits discussed.

The simplified TE process

As shown in *Figure 1*, the process consists of a single vessel that represents a combination of the reactor and separation system in the original TE process. The total volume is fixed. A single, irreversible reaction occurs in the vapour phase:

$$A + C \rightarrow D$$

A and C are non-condensable, and D is a non-volatile liquid. Feed 1 contains A, C and trace amounts of an inert, B. Feed 2 is pure A, and can compensate for disturbances in the A/C ratio in Feed 1. The solubilities of A, B and C in D are negligible. Thus, the vapour phase consists of A, B and C, and the liquid is pure D. Independent controls (not shown) maintain isothermal operation. The reaction rate depends on partial pressures of A and C only. (The original TE problem involves multiple, highly exothermic reactions that are sensitive to temperature variations, and reaction rates vary inversely with the liquid holdup in the reactor.)

The product rate, stream 4, is adjusted by a built-in proportional feedback controller (not shown) in response to variations in the liquid inventory. The purge rate, stream 3, depends on the pressure in the vessel, and on the percentage opening of the control valve in the line, which is one of the available manipulated variables. The two feed rates can also be manipulated.

Measured outputs include the flow rates of the four streams, pressure, liquid holdup volume and mole % of A, B and C in the purge. The composition measurements come from a (simulated) chromatograph, which operates on a 6 min cycle, i.e. composition measurements include a pure time delay as in the original TE problem. Between samples, the composition signals are constant.

The regulatory control problem is to maintain a specified product rate by manipulating flows of streams 1, 2 and 3. The operating pressure must be kept below the shutdown limit of 3000 kPa. There are saturation constraints on all flow rates. At a higher level, one would also like to minimize operating costs, which are a function of purge losses of A and C.

Dynamic model

Conservation laws for the chemical species give:

$$\frac{dN_A}{dt} = y_{A1}F_1 + F_2 - y_{A3}F_3 - R_D \quad [\text{kmol h}^{-1}] \tag{1}$$

$$\frac{dN_B}{dt} = y_{B1}F_1 - y_{B3}F_3 \quad (\text{kmol h}^{-1}) \tag{2}$$

$$\frac{dN_C}{dt} = y_{C1}F_1 - y_{C3}F_3 - R_D \quad (\text{kmol h}^{-1}) \tag{3}$$

$$\frac{dN_D}{dt} = R_D - F_4 \quad (\text{kmol h}^{-1}) \tag{4}$$

where N_i is the molar holdup of i in the vessel (kmol), y_{ij} is the mole fraction of i in stream j, and F_i is the molar rate of stream i (kmol h^{-1}). The production rate of D is:

$$R_D = k_0 P_A^{1.2} P_C^{0.4} \quad (\text{kmol h}^{-1}) \tag{5}$$

where $k_0 = 0.00117$ (constant for the assumed isothermal operation).

$$P_i = y_{i3}P \quad (\text{kPa}) \tag{6}$$

is the partial pressure of i in the vapour space and the purge. The system also obeys the ideal gas law:

$$P = \frac{NRT}{V_v} \quad (\text{kPa}) \tag{7}$$

where $T = 373$ K, $R = 8.314$ kJ kmol^{-1} K^{-1}, the total molar holdup in the vapour phase is

$$N = N_A + N_B + N_c \quad (\text{kmol}) \tag{8}$$

and the vapour volume is:

$$V_V = V - V_L \quad (\text{m}^3) \tag{9}$$

where $V = 122$ m^3 is the constant total volume. The liquid holdup is:

Table 1. Summary of variables and nominal operating conditions

State variable	Nominal value	Significance	Symbol	Units
x_1	44.49999958429348	Molar holdup of A	N_A	kmol
x_2	13.53296996509594	Molar holdup of B	N_B	kmol
x_3	36.64788062995841	Molar holdup of C	N_C	kmol
x_4	110.0	Molar holdup of D	N_D	kmol
x_5	60.95327313484253	Feed 1 valve position	χ_1	%
x_6	25.02232231706676	Feed 2 valve position	χ_2	%
x_7	39.25777017606444	Purge valve position	χ_3	%
x_8	47.03024823457651	Product valve position	χ_4	%

Manipulated variable	Nominal value	Purpose	Range
u_1	60.95327313484253	changes χ_1	0–100%
u_2	25.02232231706676	changes χ_2	0–100%
u_3	39.25777017606444	changes χ_3	0–100%
u_4	44.17670682730923	setpoint for y_6	0–100%

Output variable	Nominal value	Significance	Symbol	Dimensions	Range
y_1	201.43	Feed 1 flow measurement	F_1	kmol h^{-1}	0–330.46
y_2	5.62	Feed 2 flow measurement	F_2	kmol h^{-1}	0–22.46
y_3	7.05	Purge flow measurement	F_3	kmol h^{-1}	see Eq. (13)
y_4	100.00	Product flow measurement	F_4	kmol h^{-1}	see Eq. (13)
y_5	2700.00	Pressure	P	kPa	<3000
y_6	44.18	Liquid inventory	V_L	% of max	0–100
y_7	47.00	Amount of A in purge	y_{A3}	mol %	0–100
y_8	14.29	Amount of B in purge	y_{B3}	mol %	0–100
y_9	38.71	Amount of C in purge	y_{C3}	mol %	0–100
y_{10}	0.2415	Instantaneous cost	C	\$ $kmol^{-1}$	0–?

Disturbance variable	Nominal value	Significance	Dimensions
y_{A1}	0.485	Mole fraction A in Feed 1	—
y_{B1}	0.005	Mole fraction B in Feed 1	—

$$V_L = \frac{N_D}{\tilde{\rho}_L} \quad (m^3) \tag{10}$$

where the liquid molar density is $\tilde{\rho}_L = 8.3$ kmol m^{-3}, a constant. The mole fraction in the vapour phase of the vessel is the same as that in the purge, defined as:

$$y_{i3} = \frac{N_i}{N} \tag{11}$$

The molar rates of streams 1 and 2 are linear functions of valve position:

$$F_i = F_{i,max}\frac{\chi_i}{100} \text{ for } i = 1, 2 \quad (\text{kmol } h^{-1}) \tag{12}$$

where $0 \leq \chi_i \leq 100$ is the ith valve position (% open). The other two molar rates are nonlinear functions of valve position and system pressure:

$$F_i = \left(\frac{\chi_i}{100}\right) C_{vi}\sqrt{P - 100} \text{ for } i = 3, 4 \quad (\text{kmol } h^{-1}) \tag{13}$$

The nominal values of the parameters in Equations (12) and (13) are: $F_{1,max} = 330.46$ (kmol h^{-1}), $F_{2,max} = 22.46$ (kmol h^{-1}), $C_{v3} = 0.00352$, $C_{v4} = 0.0417$. Equation (13) ignores the potential effect of liquid holdup (static head) on F_4. This simplification avoids the need to define a cross-sectional area for the liquid holdup. In any case, F_4 is influenced by the liquid holdup via the inventory controller (see Equation (15)). Also, the variations in the term $\sqrt{P-100}$ are usually small (on a percentage basis) relative to the effect of the valve position. Thus, valves 3 and 4 are nearly linear.

The valve positions respond gradually to a change in a command signal, u_i, as follows:

$$\tau_v \frac{d\chi_i}{dt} = u_i - \chi_i \text{ for } i = 1,3 \quad (\%) \tag{14}$$

$$\tau_v \frac{d\chi_4}{dt} = [\bar{\chi}_4 + K_c(u_4 - y_6)] - \chi_4 \quad (\%) \tag{15}$$

where $\tau_v = 10/3600$ (h) is a valve time constant, identical for all four values. This makes the process model strictly proper; otherwise the rate measurements (which are designated as process outputs, see *Table 1*) would respond instantly to a change in the command signals. The first three manipulated variables, u_i, $i = 1,3$, are valve command signals (%), whereas u_4 is the setpoint for the proportional controller for the liquid inventory. The nominal gain of this controller is $K_c = -1.4$. The instantaneous operating cost is:

$$C = \frac{F_3}{F_4}(2.206y_{A3} + 6.177y_{C3}) \quad (\$(\text{kmol product})^{-1}) \tag{16}$$

Table 1 summarizes the eight state, four manipulated and 10 output variables, and lists nominal values for steady-state operation at the base case, where the production rate is 100 kmol/h, the pressure is 2700 kPa, the liquid inventory is about 44% of the maximum (i.e. 44% of 30 m³), and the purge contains 47 mole% A. The model parameters were chosen such that characteristic times and kinetics are similar to those in the original TE problem.

Appendix I derives a linear time-invariant (LTI) dynamic model of the plant at the base-case state, and compares its step responses with those of the nonlinear plant. These plots are one measure of model error, which could lead to robustness problems in a model-based control system. The LTI model fits well for small steps, but exhibits serious flaws as the plant moves away from the base point, as discussed in the section on steady-state characteristics.

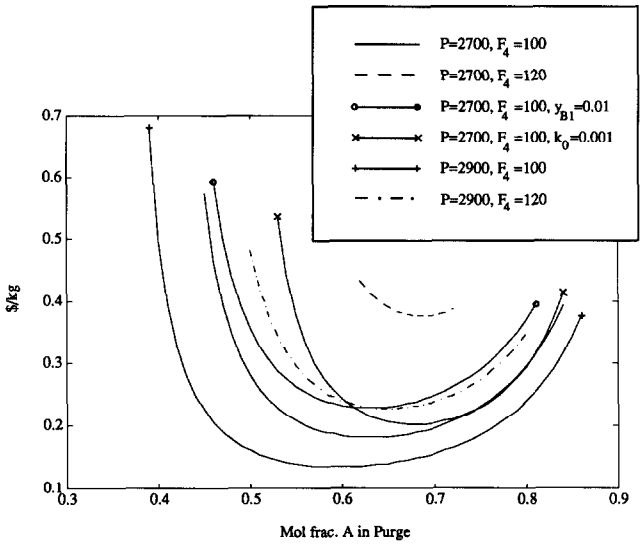

Figure 2 Operating costs as a function of operating conditions. The curves also show the feasible range of y_{A3} in each case. $y_{B1}=0.005$ and $k_0=0.00117$, unless noted otherwise

Scenarios for process control

The original TE problem includes 20 different disturbances, and requires the plant to operate at any of six steady-state conditions (corresponding to three possible product compositions, and either a nominal or maximum product rate). Constraints are often active, and large changes in the process characteristics occur as variables move from one steady-state to another. The following scenarios mimic some of these challenges:

I. *Regulation during a disturbance in feed composition.* Keep the production rate within 5% of nominal (i.e. 100 ± 5 kmol h^{-1}), while y_{A1} changes step-wise from the nominal 0.485 to 0.45. Upper bounds on pressure and liquid inventory must be satisfied at all times.
II. *Production rate increases.* Ramp production as rapidly as possible from $F_4=100$ to $F_4=130$ kmol h^{-1}, while satisfying all other constraints.
III. *Sudden loss of F_2.* When the pure A feed is unavailable, the process must operate with a stoichiometric excess of C. If possible, maintain the specified production rate. Otherwise, maximize production.
IV. *Drift in kinetic parameters.* In Equation (5), the constant of proportionality drifts from 0.00117 to 0.001, while the exponent on P_C drifts from 0.4 to 0.35. Drift is linear over a 48 h period.
V. *Change in purge concentration.* Move from nominal point ($y_{A3}=47\%$) to $y_{A3}=63\%$. One might do this in order to reduce operating costs (which are less than half those at the base point if all other factors are nominal).
VI. *Increase in inert content of Feed 1.* As for Scenario I, but y_{B1} increases from 0.005 to 0.01, with y_{A1} constant at 0.485.

Additional scenarios might include simultaneous control and optimization to reduce operating costs. The present work will focus on the control issues alone, however.

Steady-state characteristics

We now consider the impact of the plant's steady-state characteristics on the control strategy. There is flexibility in the choice of operating conditions, suggesting that the strategy should be the solution of an optimization problem. In practice, however, unmeasured disturbances and parameter drift make true optimality an elusive goal. Robust, nearly-optimal strategies are the focus of this paper.

There are four manipulated variables, suggesting that four variables can be controlled independently. Candidates for control include:

1. Production rate, F_4
2. Pressure, P.
3. Liquid inventory, V_L
4. One or more purge concentrations, y_{A3}, y_{B3}, y_{C3}.
5. Purge flow, F_3, or a purge-to-feed ratio.
6. A feed flow, or ratio of feed flows.
7. Instantaneous cost.

The first three *must* be controlled. Failure to do so will upset downstream units and/or profitability (in the case of F_4), or will allow a violation of bounds on P and V_L. The liquid inventory has no effect on steady-state operating costs, so the main focus is on P, F_4, and a fourth variable to be chosen.

As shown in *Figure 2*, it is best to run the reactor at the maximum possible pressure. (The same is true of the original TE problem). As P increases, one can tolerate a higher partial pressure of inerts, which reduces the cost of the purge (i.e. y_{A3} and y_{C3} decrease in Equation (16)). The optimal setpoint for the pressure is as close as poss-

ible to shutdown limit of 3000 kPa. A safety margin is needed to prevent an unnecessary shutdown during a disturbance. The margin size depends on the performance of the pressure control system.

Now suppose that we have selected setpoints for P, V_L and F_4. These determine the production rate and the inventories of *total* vapour and liquid. Equation (5) shows that the process is also sensitive to component inventories, and a composition variable (y_{A3}, y_{B3} or y_{C3}) would be a logical choice for the fourth controlled variable. Suppose we specify y_{A3}. This fixes y_{C3} such that $F_4 = R_D$ in Equation (5), and $y_{B3} = 1 - y_{A3} - y_{C3}$. Given the feed composition (y_{A1} and y_{B1}), one can use the steady-state versions of Equations (1)–(4) to calculate the required feed and purge flows, i.e. there is a unique steady-state. The same approach can be used if either y_{B3} or y_{C3} is specified in place of y_{A3}.

A disadvantage of composition control is that the feasible setpoint range is limited. For example, if y_{A3} is controlled and the setpoint is too low, the equations show that either the required y_{C3} is greater than unity, F_2 goes negative to satisfy material balance constraints, or F_3 hits its upper limit in an attempt to purge excess C. If y_{A3} is too high, either F_2 or F_3 exceeds its upper bound. *Figure 2* shows the feasible range of y_{A3} values for several combinations of P and F_4 (and for the nominal kinetics). For example, at the base-case of $P = 2700$ kPa, $F_4 = 100$ kmol h^{-1}, the feasible range is $0.429 \leq y_{A3} \leq 0.886$. Both limits are set by the upper bound on the purge flow. The feasible range shrinks as the production rate increases and the pressure decreases. Consider, for example, a production rate increase from the nominal $F_4 = 100$ to $F_4 = 130$. At $P = 2700$, the higher rate is feasible only for $0.685 \leq y_{A3} \leq 0.708$! A move to $P = 2850$ expands these bounds to $0.548 \leq y_{A3} \leq 0.814$, but in general, a poor choice of setpoint might make it impossible to reach the production target.

On the other hand, options 5–7 in the above list are even less attractive. An arbitrary choice of either a feed or purge flow will cause the component inventory to float as disturbances enter the system. For example, suppose we fix the purge flow. If the molar feed rate of the inert increases, y_{B3} must increase, which dilutes the reactants and reduces the production rate. Similarly, if we fix the ratio of feed flows, a change in y_{A1} distorts the reactant balance. Nor is the operating cost a good candidate for regulation. It can vary dramatically during transients and is a complex function of the system state.

Multiloop control strategies

The following development assumes that we will control one of the composition variables. The availability of the pure A feed favours y_{A3} over y_{C3}, so the choice is between y_{A3} and y_{B3}. We first consider a multiloop strategy, which requires that we pair each controlled variable with a manipulated variable. A popular way to select such pairings is to use an interaction measure, such as the relative gain array (RGA). We simplify the problem by pairing V_L with u_4 (the inventory setpoint), then considering two alternative three-input, three-output pairings. In the first, the controlled variables are F_4, P and y_{A3}, and the manipulated variables are u_1 to u_3. At the base-case steady-state, the steady-state gains are:

$$\Delta\mathbf{y} = \begin{bmatrix} \Delta F_4 \\ \Delta P \\ \Delta y_{A3} \end{bmatrix} = \begin{bmatrix} 1.6208 & 0.1369 & -0.0835 \\ 46.5606 & -36.2879 & -9.1453 \\ -0.6766 & 1.5728 & 0.0711 \end{bmatrix} \begin{bmatrix} \Delta u_1 \\ \Delta u_2 \\ \Delta u_3 \end{bmatrix} = \mathbf{K}_1\Delta\mathbf{u} \quad (17)$$

The corresponding RGA is:

$$\Lambda_1 = \mathbf{K}_1.*(\mathbf{K}_1^{-1})^T = \begin{bmatrix} 1.24 & 0.03 & -0.26 \\ -0.43 & -0.14 & 1.56 \\ 0.19 & 1.11 & -0.30 \end{bmatrix} \quad (18)$$

where '.*' denotes element-by-element multiplication of two matrices (see, e.g. Reference (9), p. 456). Based only on this information, one would conclude that the most suitable pairings are:

1. Control production rate ($y_1 = F_4$) using Feed 1 (u_1).
2. Control pressure ($y_2 = P$) using the purge rate (u_3).
3. Control A in the purge ($y_3 = y_{A3}$) using Feed 2 (u_2).

Loop 3 is an obvious pairing, but there is a serious problem with loop 2: the pressure is being regulated by the purge flow, which has a limited range. If the purge saturates, pressure control is lost unless an override mechanism is added.

The second structure replaces y_{A3} with y_{B3}. For the base-case, the gains are:

$$\Delta\mathbf{y} = \begin{bmatrix} \Delta F_4 \\ \Delta P \\ \Delta y_{B3} \end{bmatrix} = \begin{bmatrix} 1.6208 & 0.1369 & -0.0835 \\ 46.5606 & -36.2879 & -9.1453 \\ -0.12065 & 0.0997 & -0.3389 \end{bmatrix} \begin{bmatrix} \Delta u_1 \\ \Delta u_2 \\ \Delta u_3 \end{bmatrix} = \mathbf{K}_2\Delta\mathbf{u} \quad (19)$$

and the RGA matrix is:

$$\Lambda_2 = \begin{bmatrix} 0.942 & 0.089 & -0.031 \\ 0.078 & 0.863 & 0.059 \\ -0.020 & 0.048 & 0.972 \end{bmatrix} \quad (20)$$

for which the preferred pairings would be:

1. Control production rate (F_4) using Feed 1 (u_1).
2. Control pressure (P) using Feed 2 (u_2).
3. Control B in the purge (y_{B3}) using the purge rate (u_3).

Based on the RGAs, the second structure seems at least

as good as the first. There are two serious problems with the pressure control loop in this case, however. One is obvious: we are again using a flow with a limited range (F_2). Less obvious (and more serious) is that the *sign* of the loop gain changes with operating conditions. When A is in deficit, an increase in u_2 (pure A feed) *decreases* the pressure, but when A is in excess, the opposite is true. This is caused by the bimolecular form of the rate law, Equation (5), which requires significant partial pressures of both A and C at high production rates. For example, if P and F_4 are at their base-case values, but y_{A3} increases from 0.47 to 0.65 (which is near-optimal according to *Figure 2*), the gains and RGA for structure 2 are:

$$\mathbf{K}_2 = \begin{bmatrix} 1.6416 & 0.0985 & -0.0729 \\ 22.9706 & 29.7000 & -36.2201 \\ 0.2509 & -0.1163 & -0.6122 \end{bmatrix},$$

$$\Lambda_2 = \begin{bmatrix} 1.035 & -0.014 & -0.021 \\ -0.045 & 0.825 & 0.220 \\ 0.010 & 0.189 & 0.801 \end{bmatrix} \qquad (21)$$

Compared to Equation (19), both the (2,2) and (3,2) elements of $\mathbf{K}_2$ have changed sign. If P were controlled by proportional-integral (PI) feedback tuned at the base case, it would be unstable at this new operating point. (It is interesting to note that the RGA gives no obvious warning of these robustness problems. The indicated pairings are the same at both operating conditions, and the numerical values are comparable to those in Equation (20)).

Thus, structure 2 requires at least two overrides: one to control P when F_2 saturates, and the other to modify the control structure when the loop gain changes sign (or to prevent such a change). The latter would be a difficult design problem. As shown in Appendix I, the sign change occurs in the vicinity of the optimal operating condition. Moreover, the location varies in a complex way with the state variables. In practice, it would be impossible to predict exactly when the change would occur. These robustness concerns eliminate structure 2 from further consideration. An alternative would be to replace P with y_{A3} (i.e. control both y_{A3} and y_{B3}), but P has a well-defined optimal setpoint, which is not the case for the compositions.

In structure 1, on the other hand, an increase in u_2 *always* increases y_{A3}, and an increase in u_3 *always* decreases P. (The magnitudes of the gains can change by more than a factor of 2, however – see Appendix I). Structure 1 also controls y_{B3} as it adjusts the purge rate to control pressure. For example, if y_{B1} increases, B begins to accumulate, and P increases. The pressure controller then increases F_3, which simultaneously reduces the pressure and purges the excess B. In other words, structure 1 uses the available manipulated variables in a natural way to control the component inventories.

To complete the strategy for structure 1, we need to select a setpoint for y_{A3}. When one is operating near the optimal point, large variations in y_{A3} have a small impact on cost. A value of $y_{A3} = 0.65 \pm 0.05$ is nearly optimal for all six curves shown in *Figure 2*. Thus, a simple, near-optimal operating strategy would be to use a constant setpoint of $y_{A3} = 0.65$.* We also need an override to control P if u_3 saturates. There are several ways to design override mechanisms. Meadowcroft *et al.* describe a systematic approach[10]. In this case, however, the required structure of the override is clear. When u_3 saturates, u_1 must be used for pressure control. It is the only remaining variable with sufficient range (also, recall that u_2 may not be available – Scenario III). Thus, production rate must be sacrificed.

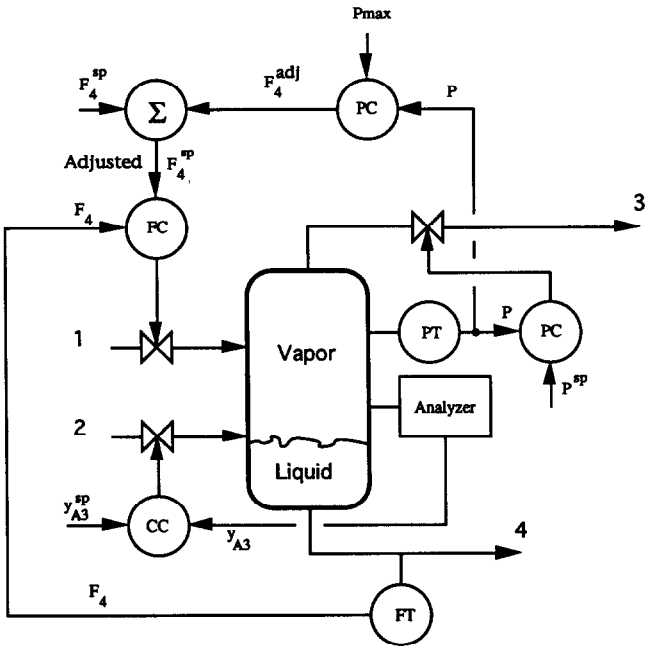

Figure 3 Multiloop control strategy. FT = flow transmitter, FC = flow controller; PT = pressure transmitter; PC = pressure controller; CC = composition controller

The override used here is a fourth feedback loop, shown in *Figure 3*. The controlled variable is the pressure, and its setpoint is a specified *maximum* pressure (which is $\geq$ the setpoint for the main pressure control loop). Its output (F_4^{adj}), which saturates at an upper bound of zero*, is a *correction* to the production rate setpoint. When it is negative (implying that P is too high), the setpoint decreases. This, in turn, causes a decrease in the main feed rate, which always reduces the pressure.

Controllers in *Figure 3* are all discrete, PI controllers with a sampling period of $\Delta t = 0.1$ h. The velocity form of the PI law was used (Reference (9), p. 196):

$$\Delta u_n = u_n - u_{n-1} = K_c\left[e_n - e_{n-1} + \frac{\Delta t}{\tau_1} e_n\right] \qquad (22)$$

where e_n = setpoint – measured value of controlled variable at sampling period n. The choice of $\Delta t = 0.1$ was determined mainly by loop 3 (which has a sampling delay of 6 min). Since the desired closed-loop time constant

*This prevents reset windup during periods when the pressure is well below the maximum.

Table 2 Controller settings for multi-loop strategy

Loop	K_c	τ_I(h)
1	0.10	1.0
2	−0.25	1.5
3	2.00	3.0
4	0.70	3.0

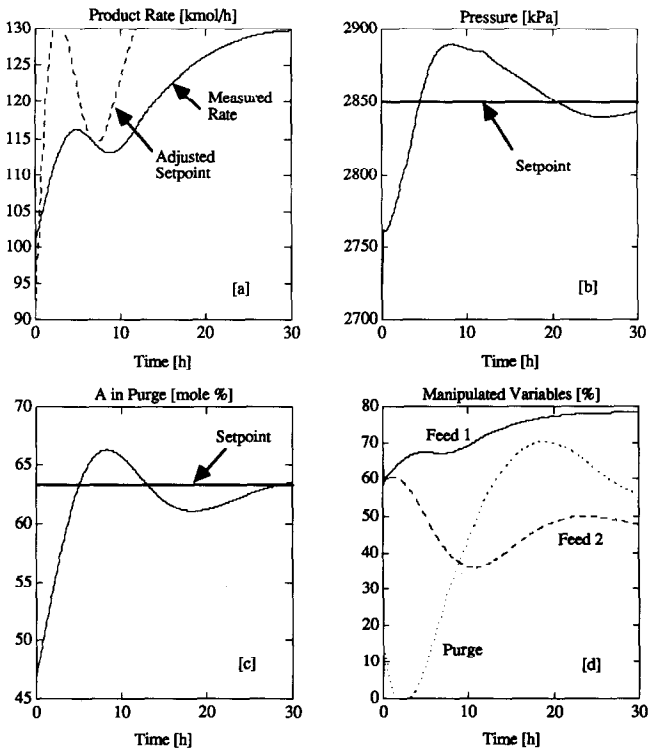

Figure 4 Multiloop control for Scenario II

was of the order of 1 h, the rules of thumb proposed by Astrom and Wittenmark[11] would suggest $\Delta t \leq 0.25$ h should be adequate. Initial values of controller gains and time constants were determined using the relay-autotuning approach (Reference (9), p.301), then adjusted by trial-and-error to reduce loop interactions where necessary. *Table 2* summarizes the final settings used in all simulations. Tuning was not difficult; even the initial values gave reasonable performance.

Figures 4–6 show the performance of this strategy for Scenarios II, III, and I, respectively. As noted previously, production of 130 kmol h^{-1} is impossible at the nominal $P = 2700$, $y_{A3} = 0.43$. Thus, for Scenario II (*Figure 4*) the setpoints of the first three loops were changed step-wise at $t = 0$ to $F_4^{sp} = 130$, $P^{sp} = 2850$, and $y_{A3}^{sp} = 0.63$. The P_{max} in the override controller (loop 4) was constant at 2900 kPa for the entire simulation.

The step changes in setpoints cause a rapid rise in P (*Figure 4b*). Loop 4 immediately decreases the production setpoint (*Figure 4a*), even though P never exceeds P_{max}. This happens because $e_n \ll e_n - 1$ in Equation (22), and the output of loop 4 is never allowed to be positive. This makes it respond immediately when the pressure exceeds the maximum, but it can also cause a premature action when pressure is increasing rapidly, as in this case.

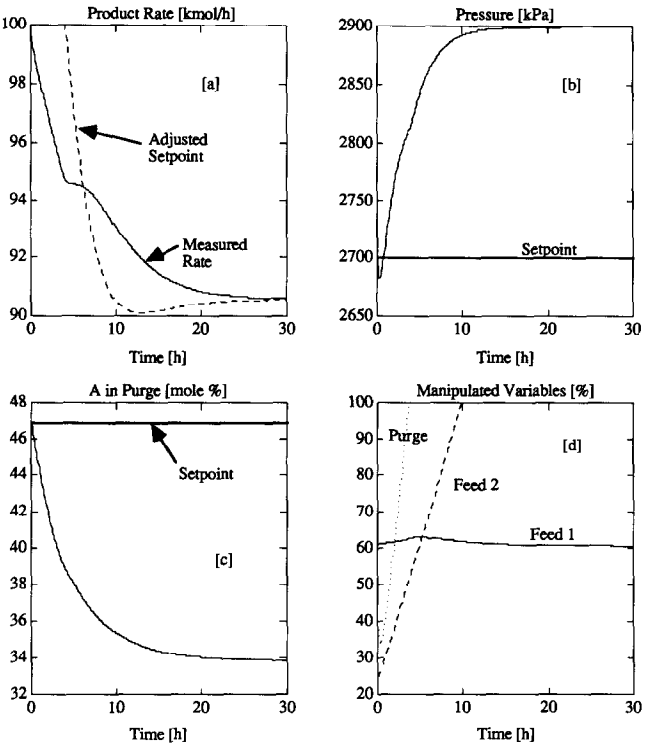

Figure 5 Multiloop control for Scenario III. Secondary feed F_2 goes to zero at $t = 0$

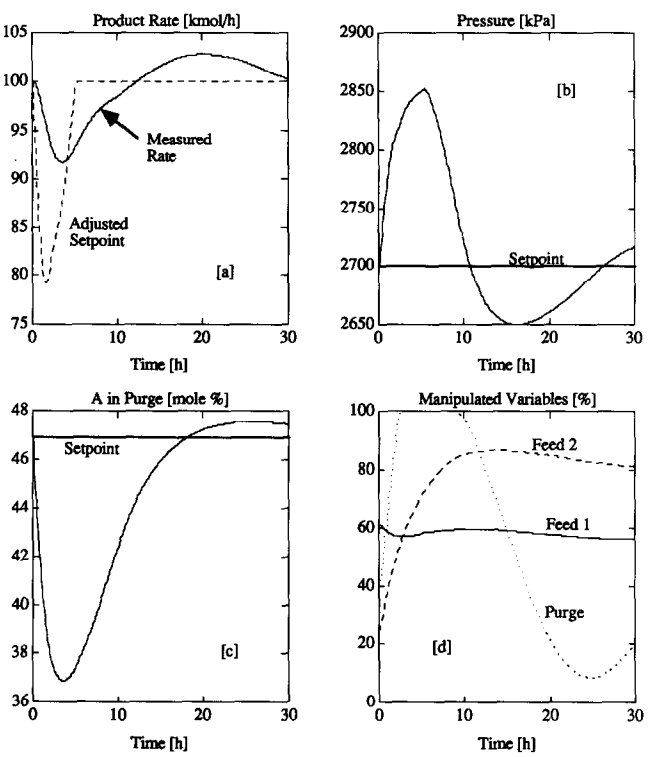

Figure 6 Multiloop control for Scenario I. A step decrease in y_{A1} occurs at $t = 0$

Note that loop 2 is simultaneously closing the purge in an effort to increase the pressure. The pressure settles temporarily (at about $t = 0.5$), so loop 4 allows the production rate setpoint to return to 130 (which happens at $t = 2$). As the production rate continues to rise, so does the pressure. It exceeds its setpoint at about $t = 4$,

and the purge valve begins to open. This is not enough to stop the pressure rise, so the production rate setpoint must again be decreased (between $t = 4$ and $t = 12$). Eventually, however, the purge valve is again able to control the pressure, and the production rate setpoint returns to 130 kPa (for $t > 12$). After 30 h, all controlled variables are at or near their setpoints.

Figure 5 shows what happens in Scenario III, when F_2 suddenly goes to zero (even though the control valve is open). All three controlled variables begin to decrease, and the loops respond accordingly (their setpoints are constant at the nominal values). The increase in u_2 (*Figure 5d*) has no effect, and y_{A3} continues to drop (*Figure 5c*). After a short time (about 0.5 h), excess reactant C has accumulated, and the pressure begins to rise (*Figure 5b*). Consequently, the purge valve reverses direction and begins to open (*Figure 5d*). When it saturates at about $t = 4$, P increases rapidly. The override controller then decreases the production rate setpoint (*Figure 5a*). At the final steady-state, both u_2 and u_3 are saturated, and loop 1 is maintaining the maximum possible production rate (with P at its specified upper bound of 2900 kPa). This is near-optimal performance for Scenario III.

In Scenario I (*Figure 6*), the sudden drop in y_{A1} (and corresponding rise in y_{C1}) at $t=0$ causes an imbalance in the reactant concentrations. Consequently, the production rate begins to drop (*Figure 6a*) and the pressure rises (*Figure 6b*). This causes the purge to saturate (*Figure 6d*), and prevents the main feed from increasing to hold the production rate. After about 4 h, however, loop 2 begins to bring y_{A3} back to its setpoint (*Figure 6c*), and the pressure stops rising. From then on, all controlled variables go smoothly back to their setpoints. The production rate falls below the stipulated minimum of 95 $kmol^{-1}$ h, but control is otherwise acceptable. The shortfall in production totals about 10 kmol over the 5 h period during which $F_4 < 95$. The nominal liquid inventory is 110 kmol. More clever use of this inventory could eliminate the drop in production. In the multiloop strategy suggested here, this would require additional logic to manipulate the setpoint on the liquid inventory, u_4 in *Table 1*. Coordination of this with the other control objectives becomes delicate and has not been attempted*. We will return to this point in the next section.

Centralized linear MPC design

The design basis is a discrete, linear, time-invariant state-space model:

$$\mathbf{x}_{k+1} = \Phi\mathbf{x}_k + \Gamma\mathbf{u}_k \tag{23}$$

$$\mathbf{y}_k = \mathbf{C}\mathbf{x}_k \tag{24}$$

*Another alternative would be to reduce the gain on the inventory controller. This would reduce variations in F_4, but would also make the process less responsive to *desired* changes in production rate.

where $\mathbf{x}_k$ is the vector of n states at sampling period k, $\mathbf{y}_k$ is the vector of n_y outputs, and $\mathbf{u}_k$ is the vector of n_u manipulated variables. For initial work, the Φ, Γ and $\mathbf{C}$ matrices were obtained from the (delay-free) LTI model in Appendix I, using a sampling period of 6 min. The delay in the purge concentration measurement was then one sampling period, and was included in the above model by augmenting the states[11].

A state estimation strategy was included to handle unmeasured disturbances. Following Wellons and Edgar[12], each output was assumed to be affected by random steps passing through a first-order system with a time constant chosen to represent the fastest disturbance. The format of the estimator was the standard Kalman filter:

$$\hat{\mathbf{x}}_{k|k-1} = \begin{bmatrix}\mathbf{x}_{k|k-1}\\ \mathbf{x}^w_{k|k-1}\end{bmatrix} = \begin{bmatrix}\Phi & \mathbf{0}\\ \mathbf{0} & \Phi^w\end{bmatrix}\hat{\mathbf{x}}_{k-1|k-1} + \begin{bmatrix}\Gamma\\ \mathbf{0}\end{bmatrix}\mathbf{u}_{k-1} \tag{25}$$

$$\hat{\mathbf{y}}_{k|k-1} = [\mathbf{C} \quad \mathbf{C}^w]\hat{\mathbf{x}}_{k|k-1} \tag{26}$$

$$\hat{\mathbf{x}}_{k|k} = \hat{\mathbf{x}}_{k|k-1} + \mathbf{L}(\tilde{\mathbf{y}}_k - \hat{\mathbf{y}}_{k|k-1}) \tag{27}$$

in which the original model has been augmented by n_w disturbance states (two for each controlled output). The matrices characterizing the disturbance dynamics were:

$$\Phi^w = \begin{bmatrix}\mathbf{I}_{n_y} & \text{diag}\{\alpha_1, \alpha_2, \ldots, \alpha_{n_y}\}\\ \mathbf{0} & \text{diag}\{\alpha_1, \alpha_2, \ldots, \alpha_{n_y}\}\end{bmatrix}; \quad \mathbf{C}^w = [\mathbf{I}_{n_y} \quad \mathbf{0}_{n_y}] \tag{28}$$

The choice of α_i determines the dynamics of the disturbance affecting y_i. For all simulations reported here, $\alpha_1 = \alpha_2 = \ldots = \alpha_{n_y} = \alpha = 0.95$. The matrix $\mathbf{L}$ is the filter gain. The steady-state solution of the Kalman filter equations for the above model gives:

$$\mathbf{L} = \begin{bmatrix}\mathbf{0}_n\\ \text{diag}\{f_1^a, f_2^a, \ldots, f_{n_y}^a\}\\ \text{diag}\{f_1^b, f_2^b, \ldots, f_{n_y}^b\}\end{bmatrix};$$

$$f_i^b = \frac{(f_i^a)^2}{1 + \alpha_i - \alpha_i f_i^a} \tag{29}$$

As explained by Lee *et al.*[13], f_i^a is a parameter that depends on the signal-to-noise ratio for the ith output. It varies between 0 and 1, where 0 implies a very noisy measurement, and 1 a very accurate measurement. As f_i^a increases, the regulatory response of the controller becomes more aggressive. A value of $f_i^a = 0.7$ was used for all outputs. In general, the estimator parameters give the designer more flexibility in shaping the servo and regulatory responses. This also increases robustness in some cases[14].

The usual quadratic version of the MPC objective function defines the optimal manipulated variable moves:

$$\min_{\Delta\mathbf{u}_k,\,\Delta\mathbf{u}_{k+1},\,\Delta\mathbf{u}_{k+P-1}} \left[\sum_{i=1}^{P}(\|\Lambda^y[\hat{\mathbf{y}}_{k+i|k} - \mathbf{r}_{k+i|k}]\|_2^2 + \|\Lambda^u\Delta\mathbf{u}_{k+i-1}\|_2^2)\right] \tag{30}$$

where P is the prediction horizon, $\Lambda^y = \text{diag}\{\lambda^y_1, \lambda^y_2, \ldots, \lambda^y_{ny}\}$, and $\Lambda^u = \text{diag}\{\lambda^u_1, \lambda^u_2, \ldots, \lambda^u_{nu}\}$, are penalties on the setpoint tracking errors and manipulated variable moves, respectively, and $\mathbf{r}_{k+i|k}$ is the vector of n_y setpoints at time $k+i$, based on information available at time k. The optimization formulation also allows upper and lower bounds on predicted outputs and manipulated variables[15]. The solution to the constrained optimization problem is obtained by quadratic programming[16].

The MPC model was a four-input, four-output system with $\mathbf{y} = [F_4, P, y_{A3}, V_L]^T$, and $\mathbf{u}$ containing the four manipulated variables listed in *Table 1*. Liquid inventory was included to reduce variations in product rate, as discussed previously. There were upper and lower bounds on V_L at 5 and 95%, and an upper bound on pressure at 2900 kPa. These bounds are, in effect, tuning parameters that include a safety margin relative to the physical constraints given in *Table 1*. Model error and disturbances make it impossible to guarantee that constraints on outputs will be satisfied. All manipulated variables were bounded at the physical limits of 0 and 100%. The prediction horizon was $P = 10$, and blocking factors for the manipulated variables were {2, 3, 5}. Penalty weights were:

$$\Lambda^y = \text{diag}\{3.0, 0.1, 1.0, 0.1\}$$

$$\Lambda^u = \lambda^u\text{diag}\{1.0, 1.0, 1.0, 2.0\}$$

with the following rationale:

- Minimize variations in production rate (relatively large penalty).
- Allow pressure to float below lower bound, and account for expected magnitude of pressure changes, which are on the order of 10 times those of the other outputs (relatively small penalty).
- Allow liquid inventory to vary if necessary (relatively small penalty).
- λ^u is a scaling factor for on-line adjustment of robustness. A large value makes the controller more cautious and thus more robust, since the system is OL-stable. The nominal value was $\lambda^u = 2$.
- Promote smooth changes in liquid inventory (relatively large penalty on u_4).

Step changes in setpoints were passed through independent first-order filters. Future values of the setpoint for use in Equation (30) were projected outputs of these filters. This is equivalent to the 'reference trajectory' used in some forms of MPC[7,17], and provides a simple way to specify the desired closed-loop response time. Filter time constants were 2.4 h for all ouputs, i.e. a desired closed-loop settling time of about 10 h.

The design is 'centralized' because it compensates for *all* interactions of the 4 × 4 system in a single controller. It works well for small changes in the setpoints and for minor disturbances, but fails dramatically for the more demanding scenarios given earlier. For example, when the setpoint on y_{A3} increases from 47 to 63% (with all other setpoints constant and no disturbances), the controller initially increases the feed rate of pure A, as expected. When the y_{A3} goes above 63%, however, the controller *continues* to increase the pure A flow until it reaches its maximum. The production rate drops rapidly, and the pressure quickly exceeds its upper bound.

This unstable response could only be prevented by increasing λ^u by more than a factor of 10, at which point performance was extremely sluggish, far inferior to that of the multiloop strategy. Even then, when P or V_L approached its bound, instability occurred. As explained by Zafiriou[18], hard output constraints take priority over penalty weights, which can often lead to such problems. Commonly used variations on the problem definition (including elimination of output constraints, changes in relative penalty weights, prediction horizon, blocking, and estimator design) were incapable of maintaining good performance of the centralized MPC strategy.

The lack of robustness is due to the gain variations described previously in the development of the multiloop strategy (see also Appendix I). The main difference is that in a MIMO strategy, a sign change in the gain of *any* transfer function can lead to instability. In this case, for example, MPC is using u_2 to control both y_{A3} and P, and the latter is causing problems when its loop gain changes. In the multiloop case we only need to worry about the gains for paired variables.

Decentralized MPC

A 'fix' in such cases is to eliminate uncertain (or troublesome) transfer functions from the model, which forces MPC to use a 'decentralized' strategy[19]. It is well known that a decentralized control structure is more robust with respect to serious modelling errors and sensor failures. Of course, this necessarily *causes* model errors, which show up as apparent disturbances in the measured outputs (and must be handled by the estimator design). Appendix II gives continuous-time transfer functions for a LTI model in which 10 of the 16 transfer functions are zero. The resulting model structure was a minor modification of that used for the multiloop design. The transfer functions were discretized with a sampling period of $\Delta t = 0.25$ h. Other MPC parameters were as given above.

Figure 7 shows the performance of decentralized MPC for a simultaneous change in the setpoints of F_4, P and y_{A3} (production rate increase, Scenario II). *Figure 4* is the same situation for multiloop control. MPC reaches the production rate target in 10 h with negligible overshoot (*Figure 7a*); it takes over 30 h in the multiloop case (*Figure 4a*). Other variables also exhibit excellent closed-loop responses. MPC has an additional degree of freedom (manipulation of liquid inventory), which allows it to respond to production rate demands more smoothly, reducing the upsets in other variables.

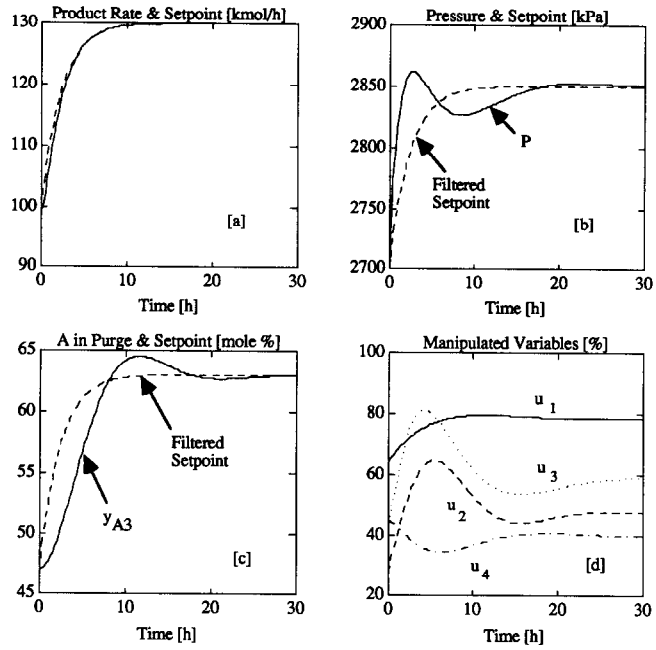

Figure 7 Decentralized MPC for Scenario II. Setpoints are filtered as explained in the text (dashed lines in a–c)

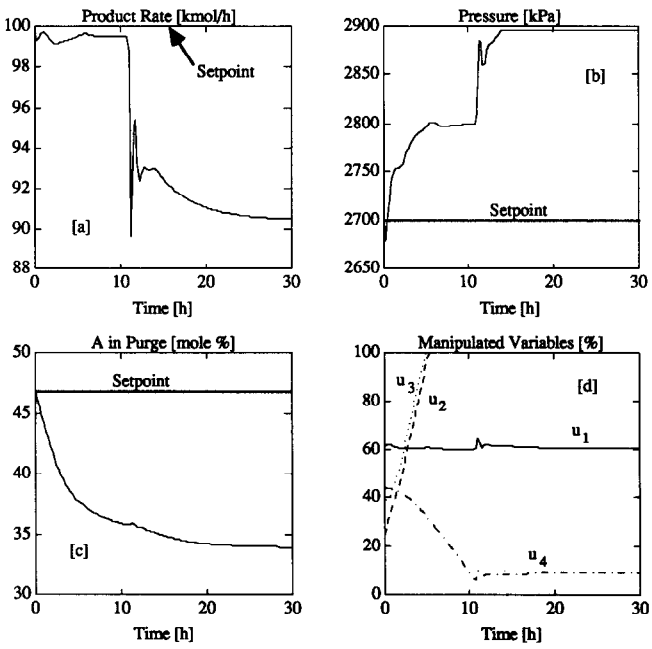

Figure 8 MPC performance for Scenario III (loss of F_2)

Similarly, for the disturbance in feed composition (shown in *Figure 6* for the multiloop case), MPC uses liquid inventory to keep the production rate within ±2.5 kmol h^{-1} of the setpoint (not shown). Recall that in *Figure 6*, production dropped about 8 kmol h^{-1} during the transient.

Figure 8 shows the constraint-handling behaviour of the MPC design for Scenario III (loss of pure A feed, F_2). Comparing *Figure 8a* and *Figure 5a*, the multiloop strategy causes a gradual drop in production rate; after 10 h it is about 93 kmol h^{-1} (the setpoint is 100). MPC, on the other hand, maintains production at about 99 kmol h^{-1} for the first 11 h by decreasing the liquid inventory. If F_2 had returned to normal during this period, a loss in production rate would have been avoided completely. Since it stays at zero, the liquid inventory eventually approaches its specified lower bound. MPC must then take drastic action to keep the vessel from running dry. *Figure 8a* shows that there is a sudden decrease in F_4 at this point. Then, according to the model used in the decentralized MPC (Appendix II), once V_L saturates the only way to influence production is via the main feed rate, F_1. Unfortunately, an increase in F_1 causes a rapid rise in the pressure, and is ultimately limited by the specified upper bound on pressure. Due to the relative weightings in Λ^y, MPC allows an offset in P in order to keep F_4 as close to 100 kmol h^{-1} as possible. Thus, the final steady-state is essentially the same as for the multiloop controller.

Whether MPC is 'better' in this case depends on the impact of step changes in F_4 on downstream equipment. If these are unacceptable, one could eliminate the constraints on V_L and increase its penalty in Λ^y, leading to behaviour similar to the multiloop response. Unfortunately, removing the constraints makes balancing the eight penalty weights more delicate. A combination that works in one scenario may not produce the desired behaviour in another. This is a basic problem with current MPC methods, and becomes more serious as the complexity of the problem increases[10]. A better approach would be to use only the first three outputs and manipulated variables in the MPC design.

Both the decentralized MPC and multiloop strategies performed adequately in the other scenarios (IV and VI – not shown). In Scenario IV, the drift in kinetics makes it impossible to make 100 kmol h^{-1} of product at the nominal pressure and purge composition. The maximum production is about 93.5 kmol h^{-1} at a pressure of 2900 kPa and a purge composition of $y_{A3}=75\%$ (where the purge rate saturates). If one holds the purge composition at the nominal 47%, the maximum production is only 73.0 kmol h^{-1} (at $P=2900$ kPa), again determined by the maximum purge flow. The required purge rate can vary dramatically in this region. For example, a 2% decrease in production allows the purge valve to go from 100% to only 64% open. In Scenario VI, the purge rate must increase, but this causes no special problems.

Discussion and conclusions

Although the process considered here is only moderately nonlinear relative to the original TE problem, performance of a centralized MPC design was unsatisfactory. Such difficulties are likely in general if one bases the design on a model of *all* the interactions in a complex, chemical process. Even rather subtle modelling errors can cause robustness problems in MIMO systems[19]. In such difficult cases it may be possible to stabilize centralized MPC through the usual tuning methods, but performance suffers. In the present work, the de-tuned cen-

tralized MPC was clearly inferior to a multiloop PI control system.

One solution, illustrated here, is to eliminate troublesome transfer functions, forcing MPC to use a decentralized strategy. A good starting point is a set of manipulated/controlled variable pairs that provide reasonable multiloop control (assuming that such pairings exist and can be identified). The MPC model would then include one transfer function (or step response) for each pair. In this limit, MPC is essentially a tuning method for multiloop control, and performance is unlikely to surpass that of a well-tuned multiloop system. Additional transfer functions may be included in the MPC design, however, to provide constant-handling features and/or compensate for well-characterized interactions.

In the present work, the only significant differences between the decentralized MPC design and multiloop PI control were for simulations involving constraints. In particular, MPC manipulated liquid inventory to reduce the impact of *temporary* disturbances on the production rate. In the case of *sustained* disturbances, however, the inventory eventually hit a constraint, and the controller then had to make sharp changes in production. If this were unacceptable (or sustained disturbances were the rule rather than the exception), it would be better to eliminate liquid inventory from the MPC design. It would then be regulated by the built-in level controller, and production rate would vary smoothly with inventory.

A complete solution would include a strategy for continuous minimization of operating costs. It is clear *a priori* that the pressure should be kept near its upper bound, but the choice of the purge concentration is nontrivial. A poor choice can make it impossible to achieve the production rate target, or inflate the operating cost. One could include cost in the MPC objective (as a controlled output), but modelling errors are likely to cause inappropriate decisions. Since there is only a single decision variable, an experimentally based search technique should work well, as long as it is insensitive to typical disturbances and measurement noise.

Another approach to the robustness issue is direct use of a nonlinear model. For MPC, one can derive a new linear model of the process at each sampling instant by linearizing a specified set of ODEs[4,5,20]. Although details have not been presented here, a successive linearization strategy *did* stabilize the centralized MPC design (i.e. the controller changed automatically to compensate for the gain variations in the process). Performance was better than with the multiloop or decentralized linear MPC designs, but the improvement was incremental. Computer time increased by an order of magnitude. Also, simulations were performed under ideal conditions, with a perfect (known) nonlinear model and good state estimates. Experience with a variety of applications suggests that shortcomings in these areas will again lead to robustness or performance problems in a centralized strategy. For example, an unanticipated drift in the reaction kinetics could cause the same gain errors that destabilized the original MPC design. A realistic test of a nonlinear model-based approach should deal with these issues, as well as the model identification problem, as one is forced to do in the original TE problem (where the model is unknown).

Finally, one could apply a general MIMO robust-control design method to the full 4×4 problem[21,19]. The difficulty here is the definition of model uncertainty such that the resulting controller meets reasonable performance standards under all conditions. (The elimination of transfer functions from the model can be viewed as a particular, problem-specific way of dealing with uncertainty.) It is possible that skilled application of such methods would improve the results given here. On the other hand, advocates of centralized, model-based techniques might find, as I did, that MIMO applications like the TE problem are formidable challenges.

In a recent review of the status of industrial process control, Downs and Doss[22] advocate heavier reliance on process understanding, aided by chemical engineering analysis and computer simulation. Longwell[23] makes similar observations. The present work reinforces the importance of the process characteristics. MPC can be tailored to these, as illustrated here, but this requires at least as much insight and effort as would be the case in a classical multiloop design.

Model availability

The process model is available as a standard S-function (FORTRAN .MEX format) for use with Matlab/Simulink. There is a compiled version for Macintosh computers. Matlab .M files used to generate the results given here are also available. To obtain any of these, send e-mail to RICKER@CHEME.WASHINGTON.EDU.

Acknowledgement

Financial support from the National Science Foundation (CTS-9214983) is gratefully acknowledged.

References

1 Prett, D. M., and Morari, M. 'The Shell Process Control Workshop', Butterworth, Boston, 1987
2 Prett, D. M., Garcia, C. E. and Ramaker, B. L. 'The Second Shell Process Control Workshop' Butterworth, Boston, 1990
3 Chylla, R. W. and Haase, D. R. 'Temperature control of semi-batch polymerization reactors' AIChE Annual Meeting, paper 24c, Chicago, 1990
4 Gattu, G. and Zafiriou E. *I&EC Res.*, 1992, **31**, 1096
5 Garcia, C. E. 'Quadratic/Dynamic matrix control of nonlinear processes: an application to a batch reaction process' Annual AIChE Meeting, San Francisco, 1984
6 McFarlane, R. C., Reineman, R. C., Bartee, J. F. and Georgakis, C. 'Dynamic simulator for a Model IV fluid catalytic cracking unit', AIChE Annual Meeting, paper 24d, Chicago, 1990
7 Caldwell, J. M. and Dearwater, J. G. 'Chemical Process Control – CPC IV', (Eds Arkun, Y. and Ray W. H.)) AIChE, New York, 1991, 319
8 Downs, J. J., and Vogel, E. F. 'A plant-wide industrial process control problem' AIChE Annual Meeting, paper 24a, Chicago, 1990

9 Seborg, D. E., Edgar, T. F. and Mellichamp, D. A. 'Process Dynamics and Control', Wiley, New York, 1989
10 Meadowcroft, T. A., Brosilow, C. and Stephanopoulos, G. 'Robustness and performance properties of modular multivariable control' Annual AIChE Meeting, Paper 4B, Chicago, 1990
11 Astrom, K. J. and Wittenmark, B. 'Computer-Controlled Systems' Prentice-Hall, Englewood Cliffs, 1984
12 Wellons, M. C. and Edgar, T. F. *Ind. Eng. Chem. Res.*, 1987, **26**. 1523
13 Lee, J. H., Morari, M. and Garcia, C. E. *Automatica*, 1993 (in press)
14 Ricker, N. L. *I&EC Res* 1990, **31** 374
15 Ricker, N. L., 'Chemical Process Control – CPC IV' (Eds Arkun, Y. and Ray, W. H.) AIChE, New York, 1991, 271
16 Morari, M. and Ricker, N. L. 'CACHE Model Predictive Control Toolbox.' CACHE Corp. V1.0, 1992
17 Grosdidier, P., Froisy, B. and Hammann, M. 'Model-based Process Control: Proceedings of the IFAC Workshop', (Eds, McAvoy, T. Arkun, Y. and Zafiriou, E.) Pergamon Press, Oxford, 1989, 31
18 Zafiriou, E. and Marchal, A. L. *AIChE J.* 1991, **37**, 1550
19 Morari, M., and Zafiriou, E. 'Robust Process Control' Prentice-Hall, Englewood Cliffs, NJ, 1989
20 Lee, J. H. and Ricker, N. L. 'Extended multi-step Kalman estimator-based nonlinear model predictive control' 1993 American Control Conf., San Francisco 389
21 Prett, D. M. and Garcia, C. E. 'Fundamental Process Control', Butterworths, Boston, 1988
22 Downs, J. J. and Doss, J. E. 'Chemical Process Control – CPC IV', (Eds Arkun, Y. and Ray, W. H.) AIChE, New York, 1991, 53
23 Longwell, E. J., 'Chemical Process Control – CPV IV' (Eds Arkun, Y. and Ray, W. H.), AIChE, New York, 1991, 445
24 Byrne, G. D., and Hindmarsh, A. C. *ACM Trans. Math. Softw.* 1975, **1**, 71

Appendix I. Linear state-space model at the nominal operating condition

The Matlab/Simulink function *linmod* was used to derive a continuous-time, linear state-space model of the plant at the nominal values of the states, inputs, and disturbance variables given in Table 1. (*linmod* calculates partial derivatives in the Taylor's expansion by finite difference. These could have been obtained analytically, but the numerical approximation is excellent in this case.) Disturbance variables were held constant. Since the plant is strictly proper, the state-space model is:

$$\frac{d}{dt}\mathbf{x} = \dot{\mathbf{x}} = \mathbf{A}\mathbf{x} + \mathbf{B}\mathbf{u} \tag{I.1}$$

$$\mathbf{y} = \mathbf{C}\mathbf{x} \tag{I.2}$$

The components of **x**, **u** and **y** are *deviations* from the corresponding values listed in *Table 1*. The constant matrices **A**, **B** and **C** (to five significant figures) are shown in *Table 3*.

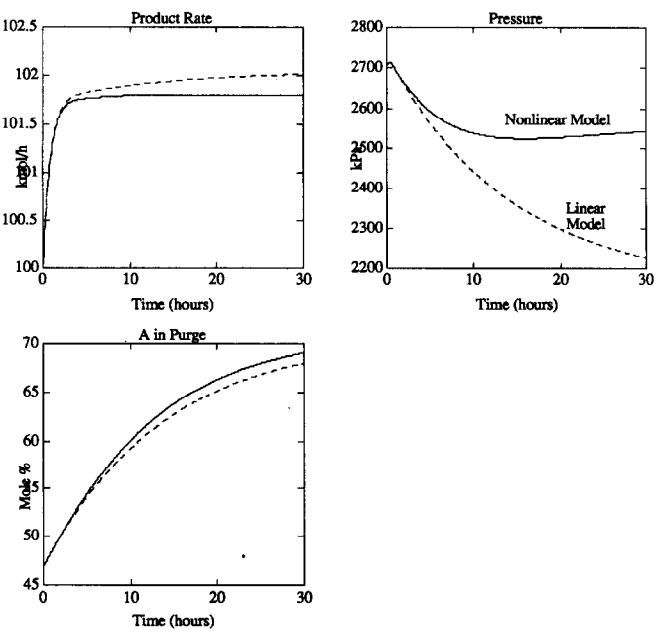

Figure I.2 Response of plant (nonlinear model) and linear state-space model to step increase of 15% in u_2

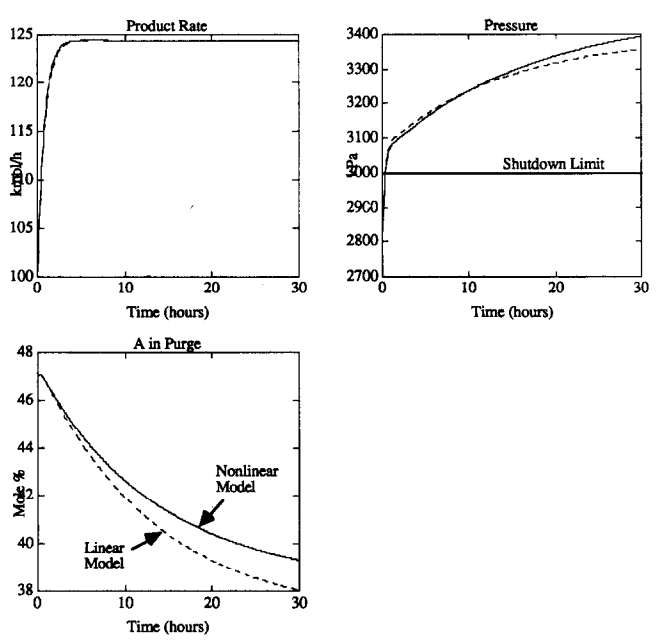

Figure I.1 Response of plant (nonlinear model) and linear state-space model to step increase of 15% in u_1

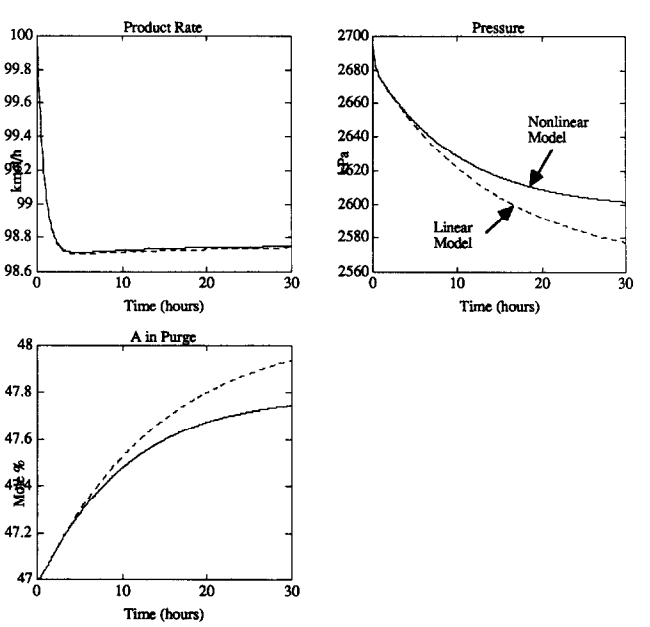

Figure I.3 Response of plant (nonlinear model) and linear state-space model to step increase of 15% in u_3

Table 3

A (columns 1–6):

−2.7542E+00	1.6816E−02	−1.0747E+00	−1.7917E−01	1.6027E+00	2.2460E−01
5.1140E−03	−6.9307E−02	5.1140E−03	−5.7936E−04	1.6523E−02	0
−2.6828E+00	1.3849E−02	−1.1520E+00	−1.7883E−01	1.6853E+00	0
2.1482E+00	−5.4840E−01	5.4307E−01	1.1974E−01	0	0
0	0	0	0	−3.6101E+02	0
0	0	0	0	0	−3.6101E+02
0	0	0	0	0	0
0	0	0	2.0298E+02	0	0

A (columns 7:8):

−8.4358E−02	0
−2.5654E−02	0
−6.9473E−02	0
0	−2.1263E+00
0	0
0	0
−3.6101E+02	0
0	−3.6101E+02

B:

0	0	0	0
0	0	0	0
0	0	0	0
0	0	0	0
3.6101E+02	0	0	0
0	3.6101E+02	0	0
0	0	3.6101E+02	0
0	0	0	−5.0542E+02

C (columns 1:6):

0	0	0	0	3.3046E+00	0
0	0	0	0	0	2.2460E−01
3.8641E−02	3.8641E−02	3.8641E−02	4.0534E−03	0	0
5.4840E−01	5.4840E−01	5.4840E−01	5.7526E−02	0	0
2.8517E+01	2.8517E+01	2.8517E+01	2.9914E+00	0	0
0	0	0	4.0161E−01	0	0
5.5978E−01	−4.9640E−01	−4.9640E−01	0	0	0
−1.5096E−01	9.0522E−01	−1.5096E−01	0	0	0
−4.0881E−01	−4.0881E−01	6.4737E−01	0	0	0
−9.0922E−04	−2.5509E−03	2.0460E−03	0	0	0

C (columns 7:8):

0	0
0	0
1.7949E−01	0
0	2.1263E+00
0	0
0	0
0	0
0	0
0	0
6.1523E−03	−5.1355E−03

The eigenvalues of **A** are −361.0108, −361.0108, −361.0108, −359.8117, −3.6418, −1.2685, −0.0702, −0.0744. There is a large separation between the fast modes (the valves) and the slower modes related to composition changes in the reactor. Thus, the ODEs are moderately stiff. They were integrated in Matlab/Simulink using a version of the EPISODE package[24], which is usually at least 30% faster than the RK45 algorithm provided in Simulink. Plots of key step responses appear in *Figs I.1* to *I.3* (for inputs 1, 2 and 3 only). These are compared to the response of the nonlinear plant model.

The linear model can be used to calculate steady-state gains[11]. *Figures I.4* to *I.7* show how the important gains vary as a function of the linearization point. To obtain these figures, LTI models were obtained over the indicated range of operating conditions. Gains were then calculated for each model. The resulting plots show large changes in gain magnitudes, with a change in sign in some cases. These are primarily responsible for the lack of robustness of the centralized MPC strategy. On the other hand, some gains are nearly constant (e.g. the response of F_4 to u_1 in *Figure I.5*).

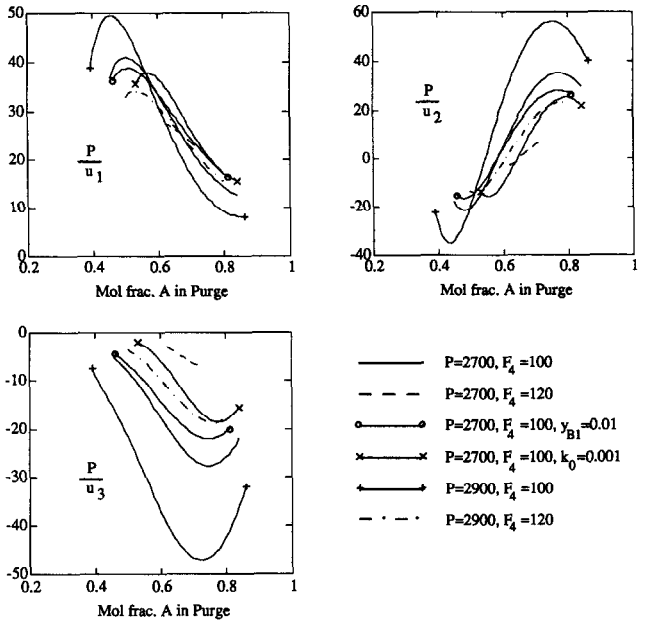

Figure I.4 Steady-state gains for response of P to u_1, u_2 and u_3 as a function of operation region. Gain units are kPa%$^{-1}$

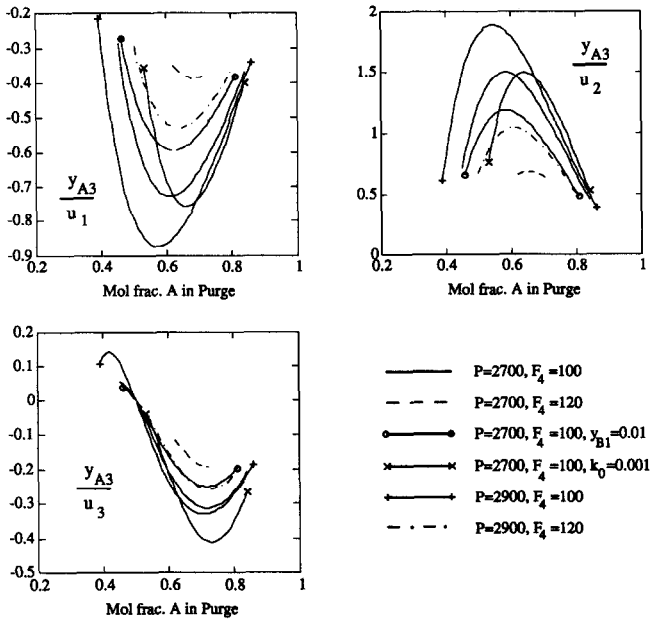

Figure I.6 Steady-state gains for response of y_{A3} (mol % A in purge) to u_1, u_2 and u_3 as a function of operation region. Gain units are % %$^{-1}$

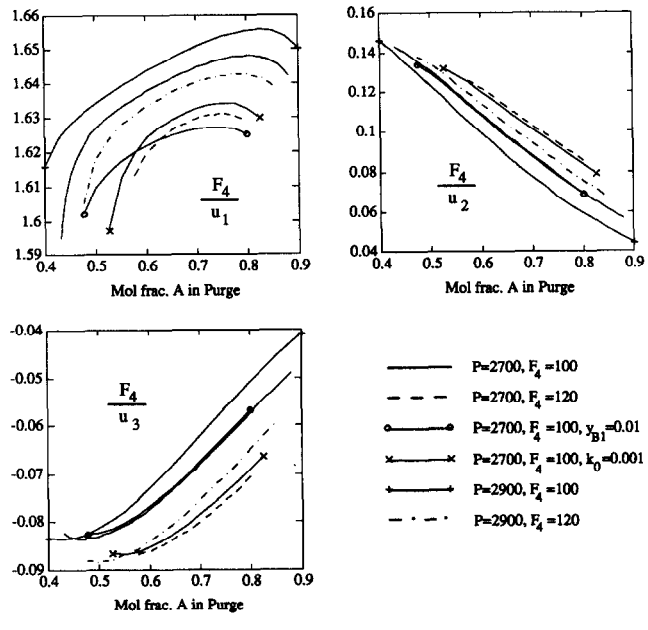

Figure I.5 Steady-state gains for response of F_4 (production rate) to u_1, u_2 and u_3 as a function of operation region. Gain units are kmol h^{-1} %$^{-1}$

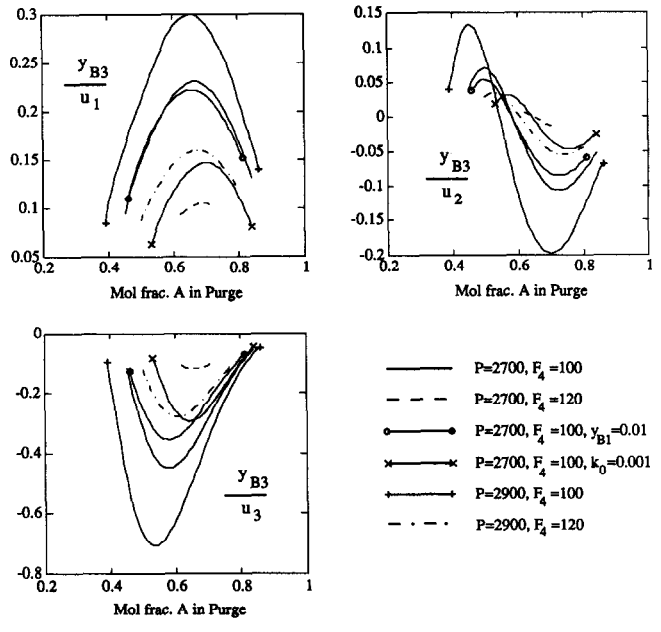

Figure I.7 Steady-state gains for responses of y_{B3} (mol % B in purge) to u_1, u_2 and u_3 as a function of operation region. Gain units are % %$^{-1}$

Appendix II. Simplified transfer-function model

To obtain a more robust MPC system, all but six of the 16 transfer functions in the model of Appendix I were set to zero. The final structure of the simplified model was:

$$\mathbf{y} = \begin{bmatrix} F_4 \\ P \\ y_{A3} \\ V_L \end{bmatrix} = \mathbf{Gu} = \begin{bmatrix} g_{11} & 0 & 0 & g_{14} \\ g_{21} & 0 & g_{23} & 0 \\ 0 & g_{32} & 0 & 0 \\ 0 & 0 & 0 & g_{44} \end{bmatrix} \begin{bmatrix} u_1 \\ u_2 \\ u_3 \\ u_4 \end{bmatrix} \tag{II.1}$$

where input and output variables are as given in *Table 1*, and the non-zero transfer functions were:

$$g_{11} = \frac{1.7}{0.75s + 1}, \quad g_{21} = \frac{45(5.667s + 1)}{2.5s^2 + 10.25s + 1},$$

$$g_{32} = \frac{1.5}{10s + 1} e^{-0.1s}, \quad g_{14} = \frac{-3.4s}{0.1s^2 + 1.1s + 1},$$

$$g_{44} = \frac{1}{s + 1} \tag{II.2}$$

These were obtained by approximating the step responses at the nominal point with a first- or second-order transfer function. The known sampling delay of 0.1 h was included in $g_{32}(s)$.

The rationale for the chosen structure is as follows. The three key elements of the multiloop strategy are g_{11}, g_{32} and g_{23}. The addition of g_{21} lets MPC control P when u_3 (the purge) saturates. The addition of g_{14} allows MPC to maintain production rate during a transient by adjusting u_4, the setpoint for the liquid inventory. We then need g_{44} to predict when the inventory will violate its upper or lower bound, and to allow MPC to move the inventory back to its nominal value when possible.